Azimuthal anchoring of liquid crystals on surfaces with high symmetry

P. C. Schuddeboom and B. Jérôme
FOM Institute for Atomic and Molecular Physics, Kruislaan 407, 1098 SJ Amsterdam, The Netherlands
(Received 22 April 1997)

Substrates with a high in-plane symmetry (threefold or higher) induce multistable anchorings in nematic liquid crystals: The preferred nematic axis in the bulk can take several equivalent orientations with different in-plane directions. To elucidate the mechanisms leading to this degeneracy, we have investigated the relation between the orientational order of cyanobiphenyl molecules at the surface of phlogopite mica plates (exhibiting a threefold symmetry) and the observed bulk orientations induced by these surfaces. In particular, in-plane bulk reorientations were observed when the system was put in the presence of water vapor. These appear to be driven by changes in the tilt distribution of the surface molecules. To account for our observations, we propose an anchoring mechanism based on the coupling of the uniaxial bulk nematic order to the surface-induced threefold order present in the first molecular layer. For this purpose the Landau–de Gennes theory of nematic liquid crystals is extended to take such a coupling into account. The calculations show that the observed in-plane bulk reorientations can be induced by changes in the surface value of the scalar nematic order parameter. [S1063-651X(97)10910-2]

PACS number(s): 61.30.Gd, 42.65.Ky, 64.70.Md

I. INTRODUCTION

A nematic liquid crystal is characterized by long-range orientational order: The usually elongated molecules are on average all aligned in a preferred direction, given by the so-called director. The particular orientation of this director is imposed by the surfaces limiting the liquid crystal or (if present) external fields. This phenomenon of orientation, or anchoring, of a liquid crystal by surfaces has been known nearly as long as have liquid crystals themselves, and numerous substrates are being developed to achieve tailored alignment patterns (see, for instance, [1–4]); however, the mechanisms by which a surface can impose this orientation in a liquid-crystalline phase are not very well understood [5].

Some progress has been made in recent years in the understanding of the anchoring on smooth surfaces such as rubbed polymer films [6–9] and mica [10–12]. In a liquid crystal in contact with surfaces, one can distinguish different regions. Right at the surface of the substrate, there is a monolayer of molecules (the surface layer; see Fig. 1) in direct interaction with the substrate. This interaction determines the orientational order of the surface layer, which therefore differs from the bulk order. As one moves away from the surface, the orientational order thus evolves from that imposed by the surface to that of the bulk. This evolution takes place in the interfacial region (Fig. 1) and results in a nematic phase with a definite orientation of the bulk director, called the anchoring direction.

In the case of the substrates mentioned above, the anchoring direction is fully determined by the nematic component of the orientational order in the surface layer [8–10]; this surface nematic order is characterized by defining a surface director as the average orientation of the surface molecules and a surface order parameter indicating the degree of alignment of these molecules along the surface director. The evolution of the orientational order in the interfacial region is well described using standard second-order Landau–de Gennes theory of the nematic phase, where the anchoring directions deduced from experimentally measured surface orientational distributions agree quantitatively with the experimental observations. The anchoring direction has the same in-plane orientation as the surface director and its tilt with respect to the surface is determined by both the tilt of the surface director and the surface order parameter.

A common characteristic of the substrates studied so far is that their surface has a mirror symmetry. Such a low symmetry allows the director in the surface layer to be either tilted or parallel to the surface. The in-plane component of the surface director introduces an in-plane anisotropy in the orientational order, with respect to which the bulk can orient.

The case of substrates with a threefold symmetry or higher [13] is different. On the one hand, they induce so-called multistable anchorings in which the bulk liquid crystal has the choice between several thermodynamically equivalent anchoring directions [5]. On the other hand, such a symmetry imposes the surface director to be perpendicular to the surface. This means that in terms of nematic ordering, the surface layer is isotropic in the plane of the surface. According to the anchoring mechanism proposed so far for low-symmetry surfaces, the bulk anchoring direction resulting

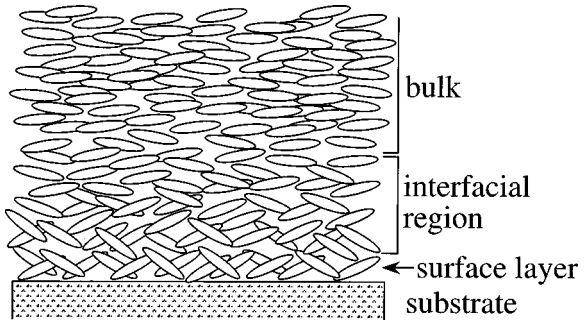

FIG. 1. Schematic representation of a liquid crystal in contact with a substrate.

from such an isotropic surface layer should have no preferred in-plane orientation (degenerate anchoring) or be perpendicular to the surface (homeotropic anchoring). However, most known examples of smooth substrates with high symmetry induce anchoring directions parallel to the substrate surface with definite in-plane orientations [14–19]. In this paper we investigate the mechanism that induces these preferred in-plane orientations on high-symmetry surfaces.

We have investigated the anchoring behavior of two cyanobiphenyl liquid crystals (5OCB and 7CB) on phlogopite mica crystals, whose surface exhibits a threefold symmetry and induces tristable planar anchorings [19]. These systems exhibit first-order anchoring transitions (i.e., discontinuous changes in anchoring directions) when water vapor is added to the atmosphere surrounding the system [19]. These transitions have been attributed to the adsorption of water molecules at the interface between the liquid crystal and the mica surface, hence their name of ''adsorption-induced'' anchoring transitions [6,7]. These transitions allow us to study different anchoring conditions in a given system and so to test the validity of the proposed anchoring mechanisms.

To investigate the anchoring behavior in these systems, we have used different experimental techniques (described in Sec. II). The anchoring directions induced by the substrate on the bulk liquid crystals have been observed using polarizing microscopy and the orientational distribution of the liquid-crystal monolayer at the substrate surface has been determined with optical second-harmonic generation. These measurements give a variation of the bulk anchoring directions and the surface orientational distribution across an anchoring transition occurring in the presence of water vapor. Our results indicate that the bulk in-plane reorientation observed at the transition is due to changes in the tilt distribution of the surface molecules (Sec. III). These observations allow us to propose an anchoring mechanism for liquid crystals on highly symmetric surfaces. This mechanism can be modeled by extending the Landau–de Gennes theory of nematic liquid crystals to take into account the surface ordering that is imposed by the substrate (Sec. IV). The correlation between anchoring directions and surface orientational order predicted by this model is in agreement with the experimental observations.

II. EXPERIMENTAL TECHNIQUES

A. Determination of bulk anchoring directions

The anchoring directions have been determined by depositing a nematic droplet and letting it spread on the mica surface. This method is based on the selection of anchoring directions by the spreading conditions of a liquid crystal on a substrate. It has indeed been shown [18,20] that when a substrate induces different possible anchoring directions, the orientation that is effectively taken by the liquid crystal depends on the direction of the spreading flow and on the contact angle between the free surface and the substrate.

During the spreading of a droplet, all the points of the nematic-substrate interface are wet under different conditions. The inside of the spread droplets is then divided into several domains where different anchoring directions have been selected. Moreover, the spreading is radial and the contact angle evolves from π when the droplet touches the substrate to zero when the droplet is completely spread. Therefore, all the wetting conditions are explored by such a spreading process and all the anchoring directions induced by the substrate are found in the droplet.

From the observation under a polarizing microscope of the texture of a nematic droplet spread on a substrate, one can deduce the following information [18,20].

(i) The number of anchoring directions induced by the substrate is half the number of domains with different orientations existing in the spread droplet.

(ii) The azimuthal orientation of the projection of the anchoring directions in the substrate plane is determined by the observation of the extinction of the different domains between crossed polarizers.

(iii) The tilt of the anchoring directions is indicated by the shape of the walls separating the domains with different orientations. In particular, planar anchorings with anchoring directions parallel to the substrate lead to radial walls. This is, however, true only for nematic liquid crystals, such as the ones used in the present study, having homeotropic anchoring conditions at the nematic-air interface, i.e., when the molecules are perpendicular to this interface.

B. Determination of surface orientational order

The orientational distribution of the surface molecules has been determined by optical second-harmonic generation. Since second-harmonic generation is forbidden in centrosymmetric media (in the electric-dipole approximation), this technique can specifically probe the polar ordering of a cyanobiphenyl surface layer [21]. The theory of second-harmonic generation by adsorbed species at substrate surfaces and its application to the determination of the orientational distribution of liquid crystal monolayers have already been described in Refs. [22,23].

Here we restrict ourselves to some features specific to our experiments. The second-harmonic signal generated by a monolayer of liquid-crystal molecules is proportional to $|\chi_{\mathrm{eff}}|^2$, where χ_{eff} is an effective nonlinear susceptibility of the monolayer dependent on the geometrical configuration used for the measurements [24]. χ_{eff} is a linear function of the nonlinear dipolar susceptibility $\overline{\boldsymbol{\chi}}$ of the liquid-crystal monolayer that can be calculated from the second-order polarizability $\overline{\boldsymbol{\alpha}}^{D}$ of one molecule. For liquid-crystal molecules such as cyanobiphenyls, $\overline{\boldsymbol{\alpha}}^{D}$ has one dominant element $\alpha^{D}_{\xi\xi\xi}$ along the long molecular axis $\hat{\boldsymbol{\xi}}$. Moreover, in our case, the phlogopite mica surface with which the liquid-crystal molecules interact has a threefold symmetry. The resulting susceptibility $\overline{\boldsymbol{\chi}}$ has only four independent nonvanishing components

$$\chi_{111}=-\chi_{122}=\tfrac{1}{4}\langle\sin^3\theta\,\cos 3\phi\rangle N_s\alpha^{D}_{\xi\xi\xi}, \tag{1a}$$

$$\chi_{112}=-\chi_{222}=\tfrac{1}{4}\langle\sin^3\theta\,\sin 3\phi\rangle N_s\alpha^{D}_{\xi\xi\xi}, \tag{1b}$$

$$\chi_{113}=\chi_{223}=\tfrac{1}{2}\langle(\cos\theta-\cos^3\theta)\rangle N_s\alpha^{D}_{\xi\xi\xi}, \tag{1c}$$

$$\chi_{333}=\langle\cos^3\theta\rangle N_s\alpha^{D}_{\xi\xi\xi}, \tag{1d}$$

where (θ,ϕ) are the spherical coordinates defining the molecular axis $\hat{\boldsymbol{\xi}}$ (Fig. 2). These components contain the information about the surface orientational distribution that is ac-

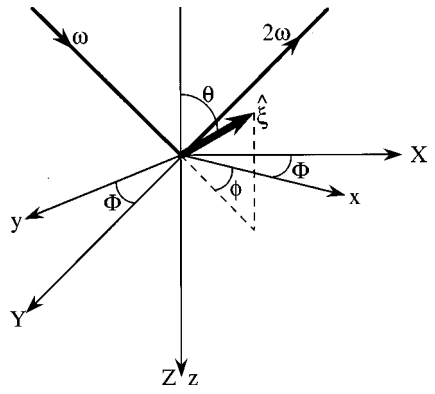

FIG. 2. Reference frames (xyz) of the substrate surface and (XYZ) of the laboratory. XZ is the incident plane of the laser beam and xz is one of the mirror planes of the substrate surface. The molecular axis $\hat{\boldsymbol{\xi}}$ is defined with respect to the substrate axes by the spherical coordinates (θ,ϕ).

cessible by second-harmonic generation. The values of the components χ_{ijk} can be obtained by measuring $|\chi_{\text{eff}}|^2$ as a function of the in-plane rotation of the sample and of the polarization s (out of the plane of incidence) or p (in the plane of incidence) of the incoming and outgoing light beams. If Φ is the angle between the plane of incidence and one of the mirror planes of the substrate (Fig. 2), the full expression of χ_{eff} for the different polarization combinations s in p out; p in, p out; p in, s out; and s in, s out is

$$\chi_{sp}=[\cos 3\Phi\chi_{122}-\chi_{222}\sin 3\Phi]\cos\vartheta L_{yy}(\omega)^2L_{xx}(2\omega)+\chi_{223}L_{yy}(\omega)^2L_{zz}(2\omega)\sin\vartheta, \tag{2a}$$

$$\chi_{pp}=[\sin 3\Phi\chi_{222}-\cos 3\Phi\chi_{122}]\cos^3\vartheta L_{xx}(\omega)^2L_{xx}(2\omega)+\chi_{223}[L_{xx}(\omega)L_{zz}(2\omega)-2L_{zz}(\omega)L_{xx}(2\omega)]\cos^2\vartheta\sin\vartheta L_{xx}(\omega)+\chi_{333}L_{zz}(\omega)^2L_{zz}(2\omega)\sin^3\vartheta, \tag{2b}$$

$$\chi_{ps}=-[\sin 3\Phi\chi_{122}+\cos 3\Phi\chi_{222}]\cos^2\vartheta L_{xx}(\omega)^2L_{yy}(2\omega), \tag{2c}$$

$$\chi_{ss}=[\sin 3\Phi\chi_{122}+\cos 3\Phi\chi_{222}]L_{yy}(\omega)^2L_{yy}(2\omega). \tag{2d}$$

ϑ is the angle of the incident and outgoing beams with respect to the surface normal (typically 45°) and $L_{ii}(\Omega)$ ($\Omega=\omega$ for the incident beam and $\Omega=2\omega$ for the second-harmonic signal) are local-field factors arising from the dielectric discontinuity of the surface. By fitting the experimental data for the different polarization configurations to these expressions, we obtain the values of the different moments χ_{122}, χ_{222}, χ_{223}, and χ_{333} of the orientational distribution function. To estimate the orientational distribution itself, we use the maximum-entropy method [25], which gives the widest distribution compatible with the measured moments.

For the samples used in the present study, the second-harmonic signal in the sp and pp polarization configurations is much stronger than the signal in the ps and ss configurations for which the second-harmonic signal produced by the mica substrate is not negligible with respect to that of a cyanobiphenyl monolayer. Since $\overline{\boldsymbol{\chi}}$ can be fully determined from the measurements of χ_{sp} and χ_{pp}, we have only used these two effective susceptibilities to calculate $\overline{\boldsymbol{\chi}}$.

We have performed our second-harmonic generation measurements in reflection using a setup similar to that already described in Ref. [21]. The incident laser beam was generated by a frequency-doubled Q-switched mode-locked neodymium-doped yttrium aluminum garnet laser (Coherent 760).

C. Samples

To prepare our samples we have used freshly cleaved phlogopite mica as the substrate. A detailed description of the structure of mica can be found elsewhere [26]. Here we give the important features that are necessary to understand the experiments described in this article. Phlogopite mica is made of a stack of sheets and cleaves easily between these sheets, which makes it possible to obtain an atomically smooth surface free of steps. The surface of these sheets exhibits a threefold symmetry with three equivalent mirror planes σ (symmetry group C_{3v}). The orientation of these planes can be determined from the cracks formed in a mica plate after perforating it with a needle and that coincide with the mirror planes σ [27].

As liquid crystals, we have used two different substituted cyanobiphenyls 7CB ($NC\Phi\Phi C_7H_{11}$) and 5OCB ($NC\Phi\Phi OC_5H_{11}$). The first one exhibits a nematic phase between 29.7 °C and 42.8 °C and the second one between 48.2 °C and 67.6 °C [28], with the possibility of supercooling the nematic phase of the latter down to 25.0 °C.

For second-harmonic generation measurements, liquid-crystal molecules were deposited onto a mica plate in the presence of a dry atmosphere by evaporating them from a hot source located 1 mm above the mica plate and letting them condense onto the plate kept at room temperature. The deposition was monitored by measuring the second-harmonic signal generated by the film. The signal first increases with time and then abruptly saturates, indicating that a full monolayer has been formed [12]. The resulting second-harmonic signal is essentially independent of the amount of liquid crystal deposited above this monolayer. This shows that this monolayer is little affected by the presence or absence of a bulk on top of it, as was already observed in other systems [24].

To study the effect of water vapor on the anchoring, the samples were placed in a chamber with a controlled atmosphere. The atmosphere composition was fixed by a slow lamellar flow of a mixture of dry nitrogen and nitrogen saturated with water vapor [29]. The composition of the atmosphere in the chamber can be characterized by the reduced partial vapor pressure $\tilde{p}=p/p_s$ of water, which is the ratio of the partial pressure p over the saturation vapor pressure p_s of water vapor. Fixing $\tilde{p}$ corresponds to fixing the chemical potential of water in the system.

III. EXPERIMENTAL RESULTS

A. Bulk anchoring directions

Both 5OCB and 7CB give spread droplets exhibiting radial walls between domains of different orientations (Fig. 3). This means that the bulk orientation for both 5OCB and 7CB

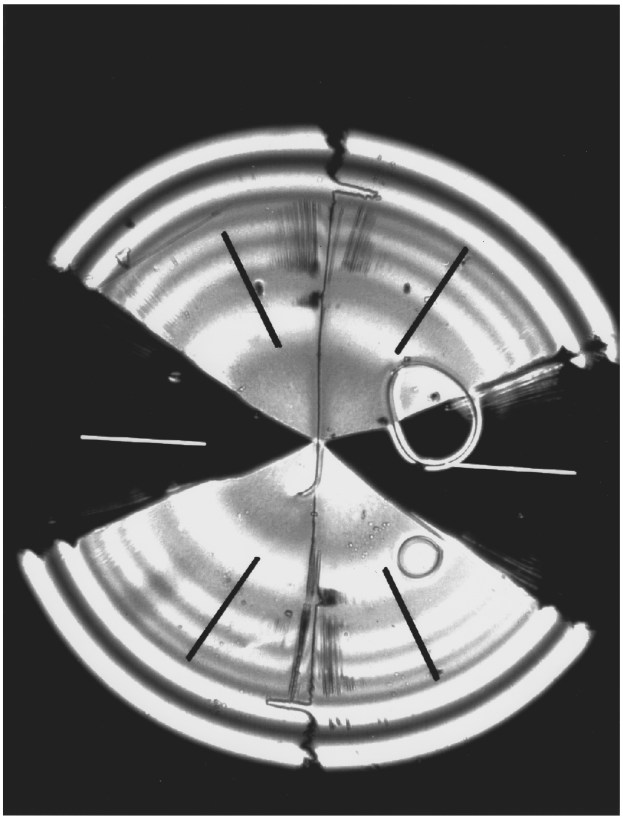

FIG. 3. Droplet of cyanobiphenyl liquid crystal deposited on phlogopite mica observed with a microscope between crossed polarizers. The bars indicate the bulk orientation in the different domains.

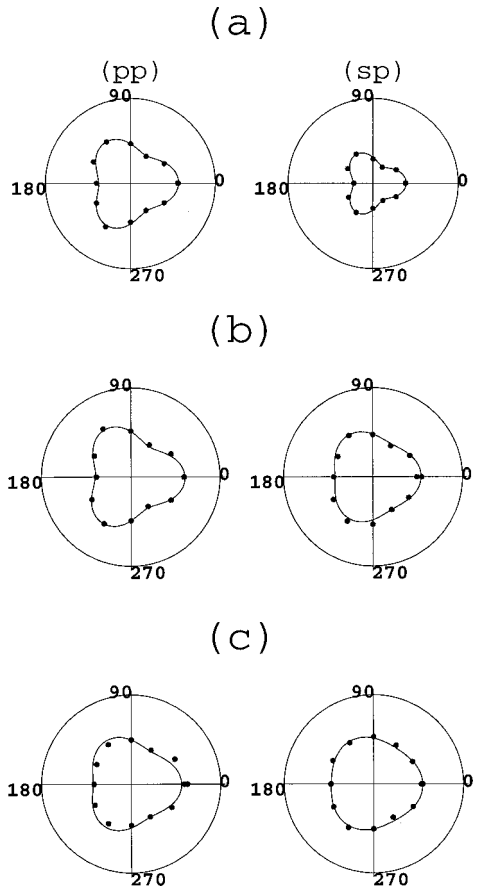

FIG. 4. Polar plots of the square root of the second-harmonic signal versus the angle Φ between the incidence plane of the laser beam and one of the mirror planes σ of the mica surface for a 5OCB film deposited on phlogopite mica in an atmosphere containing water vapor with (a) $\tilde{p}=0$, (b) $\tilde{p}=0.4$, and (c) $\tilde{p}=0.75$. The data points correspond to an average of the signal over 1200 Q-switch laser pulses. The solid lines are fits to the data points using Eq. (2).

is parallel to the surface [18,20]. The droplets contain six domains; the bulk liquid crystal has the choice between three possible anchoring directions separated by an angle of 120°, as expected from the threefold symmetry of the phlogopite mica surface.

As the water vapor pressure increases, anchoring transitions are observed that are characterized by a bulk reorientation in the plane parallel to the substrate. 5OCB and 7CB differ in the in-plane orientation of the anchoring directions. In an atmosphere of dry nitrogen, 5OCB orients perpendicular to one of the mirror planes σ of the mica surface. When water vapor is added, this system exhibits a first-order anchoring transition at a given reduced partial vapor pressure $\tilde{p}_1$ of water. At this transition, the orientation of the nematic phase jumps abruptly to a direction parallel to σ. In contrast, 7CB orients parallel to σ in a dry atmosphere, while it orients perpendicular to σ after the anchoring transition.

B. Surface orientational order

Figures 4 and 5 show the polar plots of the square root of the second-harmonic signal generated respectively by a monolayer of 5OCB and 7CB on phlogopite mica, as a function of the in-plane rotation angle Φ [Eq. (2)] for different partial water vapor pressures. In all cases, the shape of the plots shows a threefold symmetry, indicating that the surface liquid-crystalline layer follows the symmetry of the substrate. The maxima of the signal correspond to the same in-plane rotation for both 5OCB and 7CB, but the in-plane anisotropy is stronger for 7CB.

The general trend in both sets of plots is that, as the partial pressure of water vapor is increased, the anisotropy decreases. Moreover, the maxima in the plots corresponding to the sp polarization configuration increase for 5OCB and decrease for 7CB. All these changes are reversible provided the system has not been exposed to water vapor for more than approximately a day.

Figures 6 and 7 show the resulting orientational distribution functions of the surface liquid-crystal molecules. For both liquid crystals and for all pressures, the distribution exhibits four peaks from which one is pointing downward, corresponding to molecules pointing with their cyano group away from the surface. The other three peaks lie on a cone around the z axis with an opening angle of approximately 58° and in the mirror planes σ of the substrate.

In agreement with the decrease of in-plane anisotropy in the second-harmonic signal (Figs. 4 and 5), one observes in these distributions that the width of the peaks increases when the water vapor pressure increases. However, the in-plane orientation of the peaks is independent of the liquid crystal and of the composition of the atmosphere. This is in contrast

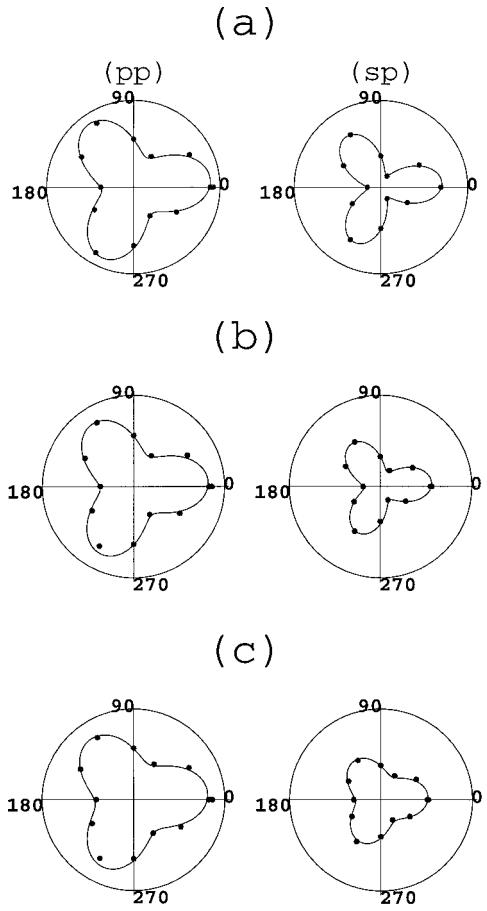

FIG. 5. Same as Fig. 4, but for 7CB with (a) $\tilde{p}=0$, (b) $\tilde{p}=0.4$, and (c) $\tilde{p}=0.75$.

with the strong variations of the bulk anchoring directions on these parameters.

To quantify the detailed evolution of the surface orientational order with water vapor pressure, we have calculated the evolution of the different order parameters characterizing the surface orientational order. The number of independent order parameters can be reduced to three: two parameters for the threefold component of the ordering,

$$Q_{111}\left\langle \frac{\cos 3\phi \, \sin^3\theta}{4} \right\rangle,$$

$$Q_{333}\left\langle \frac{3\cos\theta}{20}+\frac{\cos 3\theta}{4} \right\rangle,$$

and one parameter characterizing the nematiclike uniaxial ordering,

$$Q_{33}=\left\langle \frac{3\cos^2\theta-1}{2} \right\rangle.$$

Q_{111} is associated with the anisotropic in-plane ordering and Q_{333} is a measure of the up-down asymmetry along the surface normal. Q_{33} is the usual scalar order parameter of the nematic order indicating how well the molecules are aligned along the surface normal. In both liquid-crystalline compounds, the value of Q_{111} increases with increasing vapor pressure, while the values of Q_{333} and Q_{33} decrease in 5OCB and increase in 7CB, with, in both cases, a change of sign for Q_{33} (Fig. 8).

C. Interpretation of experimental results

From the above experimental results, we can draw several conclusions concerning the anchoring behavior of cyanobiphenyl molecules on phlogopite mica. First of all, the surface layer of liquid-crystalline molecules exhibits the symmetry of the substrate surface, namely, a threefold symmetry. This is shown by the measured second-harmonic signal (Figs. 4 and 5). However, these measurements cannot exclude the presence of a small asymmetry between the peaks of the orientational distribution, which would be hidden by statisti-

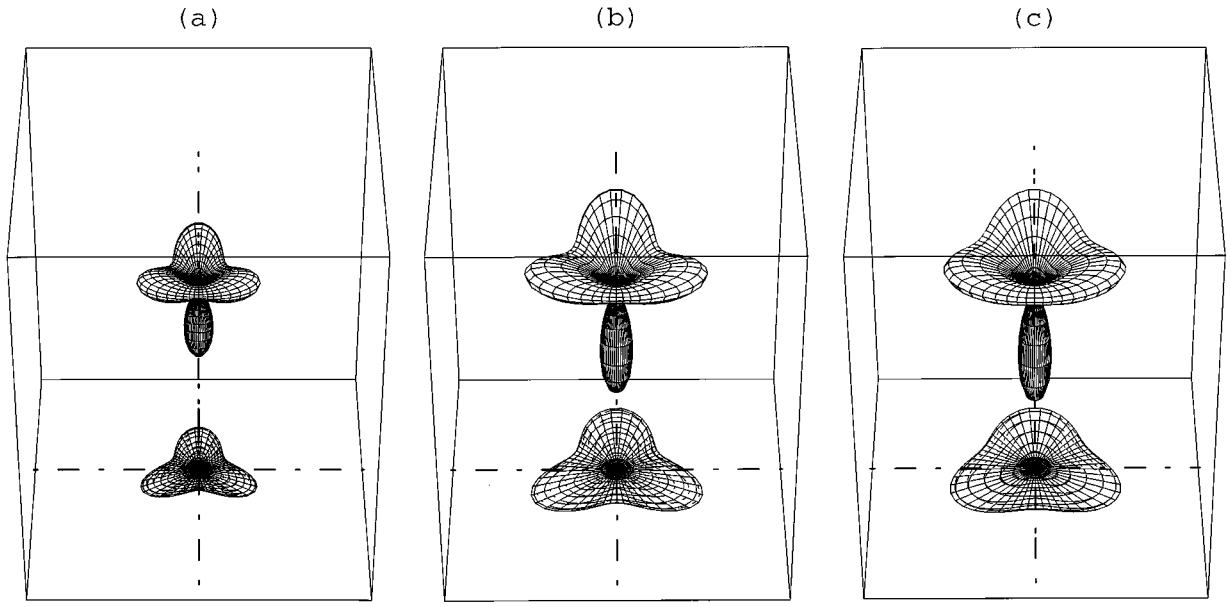

FIG. 6. Evolution of the orientational distribution $f(\theta,\phi)$ in a monolayer of 5OCB liquid-crystal molecules on a substrate of phlogopite mica, for different partial water vapor pressures (a) $\tilde{p}=0$, (b) $\tilde{p}=0.4$, and (c) $\tilde{p}=0.75$.

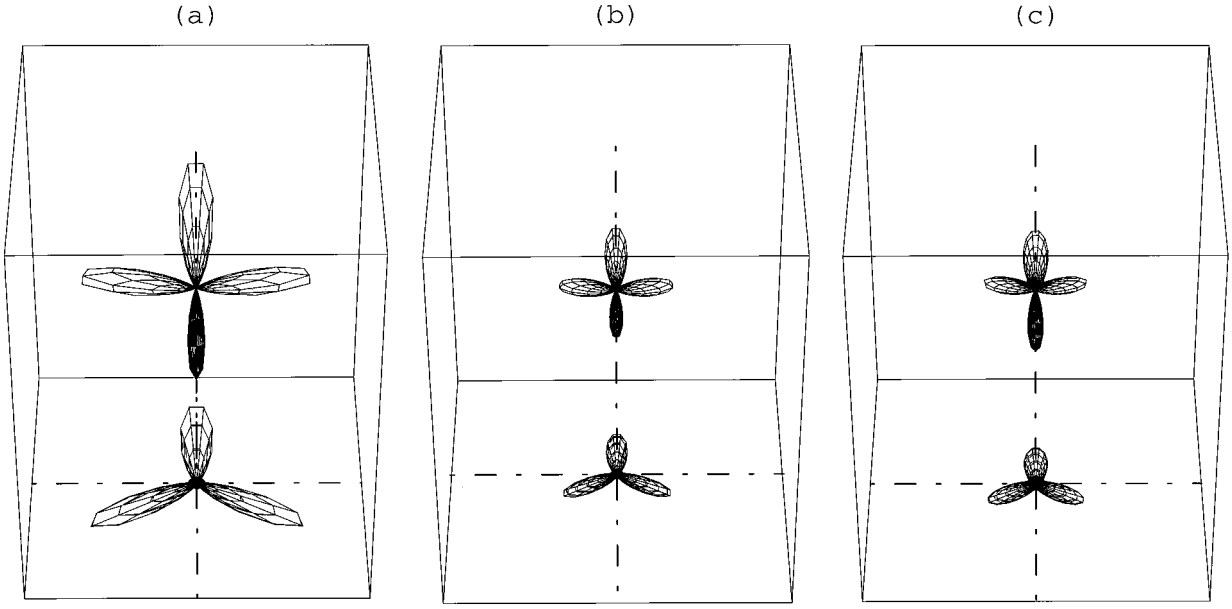

FIG. 7. Same as Fig. 6, but for 7CB different partial water vapor pressures (a) $\tilde{p}=0$, (b) $\tilde{p}=0.4$, and (c) $\tilde{p}=0.75$.

cal errors in the second-harmonic generation measurements. This possibility can be excluded by considering the fact that both liquid crystals used in our study orient in the bulk perpendicular to the surface-preferred molecular orientations under the appropriate water vapor pressure. If there was any asymmetry making one of the peaks in the surface orientational distribution larger than the others, the bulk would necessarily orient along this direction and the bulk anchoring directions would always be parallel to the preferred orientations of the surface molecules.

Second, we find that the difference in the in-plane orientation of the bulk anchoring directions that is observed between 5OCB and 7CB, before and after the anchoring transitions, is not due to a difference in the preferred in-plane orientation of the surface molecules. This is in contrast to what was found on muscovite mica [11,12]. By considering the evolution of the order parameter Q_{111} in the surface layer (which is related to the in-plane width of the peaks of the orientational distribution), it seems unlikely that the bulk orientation is affected by the in-plane distribution of the surface molecules: Q_{111} increases with increasing water vapor pressure in both 7CB and 5OCB, while the bulk anchoring directions vary in the opposite ways in these two compounds. Such an opposite behavior of 5OCB and 7CB is found in the evolution of the two order parameters Q_{333} and Q_{33} characterizing the tilt distribution of the surface molecules. This strongly suggests that the in-plane orientation of the bulk director is determined by the tilt distribution of the surface molecules. In particular, the in-plane rotation of the bulk orientation occurring at the anchoring transition induced by the addition of water vapor appears to be driven by changes in the surface tilt distribution.

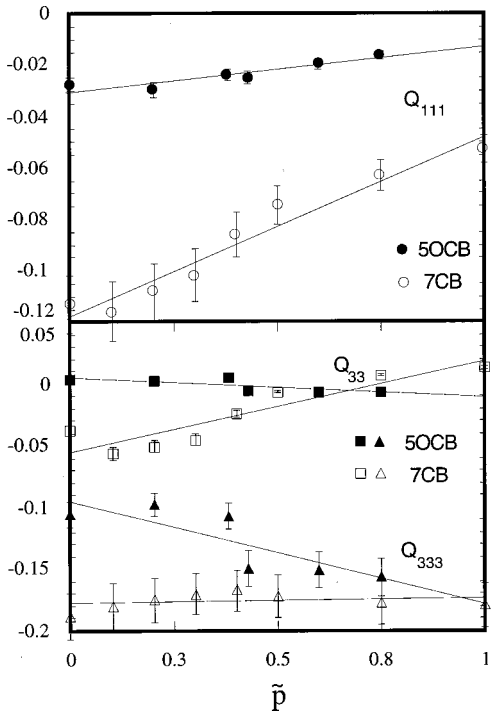

FIG. 8. Surface order parameters versus the reduced water vapor pressure $\tilde{p}$ for 5OCB and 7CB: Q_{111}, Q_{333}, and Q_{33}.

IV. THEORETICAL DESCRIPTION

In this section we develop a theoretical model accounting for our experimental observations of the anchoring behavior of cyanobiphenyl liquid crystals on phlogopite mica. Starting from these observations, we derive a possible anchoring mechanism by which the bulk liquid crystal adopts the observed definite anchoring directions in the plane of the surface. We then formalize this mechanism by extending the Landau–de Gennes theory to take into account the specific ordering induced by the substrate close to its surface.

A. Principles

On the one hand, the second-harmonic generation experiments have shown that the orientational ordering in the surface layer of molecules in contact with the mica surface exhibits the same symmetry as the substrate, namely, a

threefold symmetry. On the other hand, the orientational ordering of the bulk nematic liquid crystal is uniaxial. There are therefore two components of the molecular orientational order that play a role at the interface: the nematic ordering and the surface-induced threefold ordering. The threefold ordering disappears as one moves away from the surface layer into the bulk. The degree of nematic order is low in the surface layer, as shown by the low values of the surface order parameter Q_{33}; this nematic order grows as one moves into the bulk.

The director in the bulk of the liquid crystal has three preferred orientations parallel to the substrate surface, either parallel or perpendicular to the mirror planes of this surface (depending on the system considered). However, in the surface layer the in-plane symmetry of the orientational order imposes the director to be perpendicular to the substrate surface. This means that the boundary conditions of the nematic order are isotropic in the plane. Therefore, the nematic order cannot orient its director in a particular in-plane direction by itself, as it grows in the interfacial region. It needs to get its orientation from the only source of anisotropy in the boundary conditions, which is the component of the order with a threefold symmetry. This implies that the nematic and the threefold component of the orientational order have to be coupled. Considering the correlation that we find experimentally between the tilt distribution of the molecules in the surface layer and the in-plane orientation of the bulk director, this coupling between nematic and threefold orientational order must be such that changes in the surface tilt distribution can induce an in-plane reorientation of the bulk director.

In the following sections we model this anchoring mechanism and the evolution of the orientational order from the surface layer towards the bulk using a Landau type of description. We introduce two different order parameters describing the two different types of ordering involved in the anchoring process. These order parameters characterize the degree of ordering as well as the overall orientation of the corresponding orientational distributions. They are therefore tensors, of second rank for the nematic order [Eq. (3)] and third rank for the threefold order [Eq. (11)].

The evolution of the orientational order in the interfacial region is determined by the set of trajectories of the order parameters for which the free energy is minimal. We use an expansion of the free energy of the system in these order parameters of the form $F_{\mathrm{tot}}=F_2+F_3+F_C$. F_2 is the contribution associated with the nematic ordering, given by the Landau–de Gennes theory [30] [see Eq. (7)]. F_3 is the contribution associated with the threefold ordering. We write it as a development in the third-rank order-parameter tensor in the spirit of the Landau–de Gennes free energy [Eq. (14)]. The effect of the threefold ordering on the nematic order is taken into account by introducing the coupling term F_C written as a contraction of the two considered order-parameter tensors [Eq. (21)].

The influence of the coupling term F_C on the evolution of the nematic and threefold order is considered to be small. In our calculations we therefore treat the evolution of these different types of order independently (in Secs. IV B and IV C for the nematic and threefold order, respectively) and the coupling term as a perturbation (Sec. IV D).

B. Evolution of the nematic ordering

To describe the nematic order in the framework of the Landau–de Gennes theory, we define the z-dependent order-parameter tensor (see [30])

$$Q_{ij}(z)=\left\langle \tfrac{1}{2}(3\xi_i\xi_j-\delta_{ij})\right\rangle=\tfrac{1}{2}\int 3\xi_i\xi_j f(\theta,\phi,z)\,d\Omega-\delta_{ij}, \tag{3}$$

where $\hat{\xi}$ is the molecular orientation $(-\cos\phi\sin\theta,\sin\phi\sin\theta,\cos\theta)$, $f(\theta,\phi,z)$ is the distribution of these molecular orientations at distance z from the surface, and $d\Omega=\sin\theta\,d\theta\,d\phi$ is an elementary solid angle. We choose for convenience the frame of reference $(\hat{\mathbf{x}}\hat{\mathbf{y}}\hat{\mathbf{z}})$ in such a way that the director stays in the $\hat{\mathbf{x}}\hat{\mathbf{z}}$ plane. In that case Q_{ij} can be written as

$$\begin{bmatrix} -Q_{22}-Q_{33} & 0 & Q_{13} \\ 0 & Q_{22} & 0 \\ Q_{13} & 0 & Q_{22} \end{bmatrix}. \tag{4}$$

In the bulk this order parameter has the form

$$\begin{bmatrix} \dfrac{Q_b(1-3\cos2\Theta)}{4} & 0 & \dfrac{3Q_b\sin2\Theta}{4} \\ 0 & -\dfrac{Q_b}{2} & 0 \\ \dfrac{3Q_b\sin2\Theta}{4} & 0 & \dfrac{Q_b(1+3\cos2\Theta)}{4} \end{bmatrix}, \tag{5}$$

where Θ is the angle between the bulk director and the z axis perpendicular to the substrate surface and Q_b is the bulk scalar order parameter (approximately 0.6). At the surface Q_{ij} takes the form

$$\begin{bmatrix} \dfrac{-Q_{33}|_{z=0}}{2} & 0 & 0 \\ 0 & -\dfrac{Q_{33}|_{z=0}}{2} & 0 \\ 0 & 0 & Q_{33}|_{z=0} \end{bmatrix}. \tag{6}$$

In this case, the director is perpendicular to the surface.

The Landau–de Gennes free-energy density associated with the nematic ordering can be written as [30]

$$F_2(z)=\sum_{i,j=1}^{3}\left[\frac{A_q}{2}(Q_{ij}-Q_{b,ij})^2+\frac{l_1}{2}\left(\frac{\partial Q_{ij}}{\partial z}\right)^2+\frac{l_2}{2}\left(\frac{\partial Q_{i3}}{\partial z}\right)^2\right], \tag{7}$$

where summation over repeated indices is assumed. This free-energy density is minimal when $Q_{ij}=Q_{b,ij}$ and $\partial Q_{ij}/\partial z=0$, i.e., for a uniformly ordered bulk. It is nonzero only in the interfacial region; its integration over the semi-infinite space occupied by the liquid crystal ($z<0$) yields the interfacial energy.

We insert Eqs. (4) and (5) in the free-energy expansion (7) and perform for convenience the substitution $g(z)=2Q_{22}(z)+Q_{33}(z)$. We also introduce constants that are re-

lated to the characteristic decay lengths of the components Q_{ij}: $\xi_1=\sqrt{l_1/A_q}$, $\xi_2=\sqrt{(3l_1+2l_2)/3A_q}$, and $\xi_3=\sqrt{(2l_1+l_2)/2A_q}$. For numerical calculations we use the same value for the constants l_1, l_2, and A_q as in [10]: $l_1/l_2=2/5$ and $A_q/l_2=0.01\ \mathrm{nm}^{-2}$. $F_2(z)$ can now be written as

$$\frac{F_2(z)}{A_q}=\frac{3}{4}Q_b^2-\frac{3}{2}Q_{13}(z)Q_b\sin2\Theta+Q_{13}(z)^2+Q_{13}(z)'^2\xi_3^2-\frac{3Q_b}{8}(1+3\cos2\Theta)Q_{33}(z)+\frac{3Q_{33}(z)^2}{4}+\frac{3Q_{33}(z)'^2}{4}\xi_2^2+\frac{3}{8}Q_b(1-\cos2\Theta)g(z)+\frac{g(z)^2}{4}+\frac{g(z)'^2}{4}\xi_1^2. \tag{8}$$

By solving the corresponding Euler-Lagrange equations with Eqs. (5) and (6) as boundary conditions for, respectively, the bulk ($z=-\infty$) the and surface layer ($z=0$), we find

$$Q_{13}(z)=-\frac{3Q_b}{4}(\exp[z/\xi_3]-1)\sin2\Theta, \tag{9a}$$

$$Q_{33}(z)=\exp[z/\xi_2]Q_{33}|_{z=0}+\frac{Q_b}{4}(1-\exp[z/\xi_2])(1+3\cos2\Theta), \tag{9b}$$

$$g(z)=\frac{3Q_b}{2}(\exp[z/\xi_1]-1)\sin^2\Theta. \tag{9c}$$

From this z dependence of Q_{ij}, we can calculate the interfacial energy $\mathcal{F}_2$ whose minima correspond to the anchoring directions

$$\mathcal{F}_2=\int_{-\infty}^{0}\frac{F_2}{A_q}dz=\left\{\frac{27Q_b^2}{128}\xi_1+\frac{33Q_b^2}{128}\xi_2-\frac{3Q_bQ_{33}|_{z=0}}{8}\xi_2+\frac{3(Q_{33}|_{z=0})^2}{4}\xi_2+\frac{9Q_b^2}{32}\xi_3+\left(-\frac{9Q_b^2}{32}\xi_1+\frac{9Q_b^2}{32}\xi_2-\frac{9Q_bQ_{33}|_{z=0}}{8}\xi_2\right)\cos2\Theta+\left(\frac{9Q_b^2}{128}\xi_1+\frac{27Q_b^2}{128}\xi_2-\frac{9Q_b^2}{32}\xi_3\right)\cos4\Theta\right\}. \tag{10}$$

A contour plot of $\mathcal{F}_2$versus the surface scalar order parameter $Q_{33}|_{z=0}$ and the bulk tilt Θ shows that the preferred orientations of the director are parallel ($\Theta=\pi/2$) or perpendicular ($\Theta=0$) to the surface depending on $Q_{33}|_{z=0}$ (Fig. 9). The bulk director is parallel to the surface when the stability condition $\partial^2\mathcal{F}(\Theta,Q_{33}|_{z=0})/\partial\Theta^2|_{\Theta=\pi/2}>0$ is satisfied, which means that $Q_{ij}|_{z=0}<Q_b[(2\xi_3-\xi_2-\xi_1)/2\xi_2]\approx0.0676$. We have found experimentally that $Q_{33}|_{z=0}$ is always smaller than 0.02 (see Fig. 8); this means that the planar anchoring is stable, which corresponds to the experimental observation. In the following we consider ony the case $\Theta=\pi/2$.

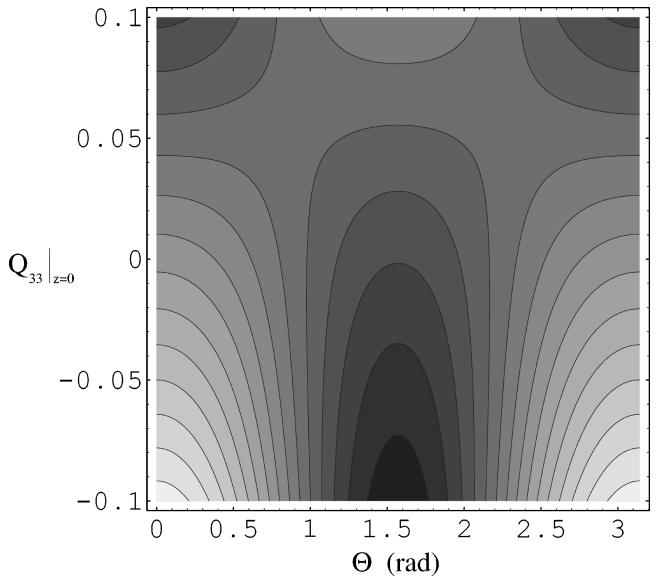

FIG. 9. Contour plot of the contribution $\mathcal{F}_2$ to the interfacial energy as a function of the surface scalar order parameter $Q_{33}|_{z=0}$ and the angle Θ of the bulk director with respect to the z axis.

C. Evolution of the threefold ordering

We proceed with the evolution of the threefold ordering as with the nematic ordering. For this we need an order parameter describing this type of ordering and terms in the free energy that determine the evolution of the components of this order parameter as a function of z.

As an order parameter we take a traceless symmetric third-rank tensor defined as

$$Q_{ijk}(z)=\int[\xi_i\xi_j\xi_k-1/5(\xi_i\delta_{jk}+\xi_j\delta_{ik}+\xi_k\delta_{ij})]f(\theta,\phi,z)d\Omega. \tag{11}$$

$Q_{ijk}|_{z=0}$ has to satisfy the threefold symmetry of the surface layer. Moreover, there is no spontaneous symmetry breaking away from the surface and thus the tensor $Q_{ijk}(z)$conserves the threefold symmetry it has in the surface layer for any z [31]. This threefold symmetry reduces the number of independent nonvanishing of components of $Q_{ijk}$to three:

$$Q_{122}(z)=-Q_{111}(z)=-\left\langle\frac{\cos3\phi\,\sin^3\theta}{4}\right\rangle, \tag{12a}$$

$$Q_{222}(z)=-Q_{112}(z)=-\left\langle\frac{\sin3\phi\,\sin^3\theta}{4}\right\rangle, \tag{12b}$$

$$Q_{223}(z)=Q_{113}(z)=-Q_{333}(z)/2=-\left\langle\frac{3\cos\theta}{40}+\frac{\cos3\theta}{8}\right\rangle. \tag{12c}$$

$Q_{122}(z)$ and $Q_{222}(z)$ describe the anisotropy in the plane and depend on the angle Ψ between the $\hat{\mathbf{x}}\hat{\mathbf{z}}$ plane containing the director and one of the mirror planes σ of the substrate surface. These components can be written as

$$Q_{122}(z)=\cos3\Psi h(z), \tag{13a}$$

$$Q_{222}(z) = -\sin 3\Psi h(z). \tag{13b}$$

We construct an expansion of the free-energy density as a function of Q_{ijk} in a way similar to the Landau–de Gennes expansion in the second-rank nematic order parameter [32]:

$$F_3(z) = \sum_{i,j,k=1}^{3} \left[\frac{A_1}{2}(Q_{ijk})^2 + \frac{\lambda_1}{2}\left(\frac{\partial Q_{ijk}}{\partial z}\right)^2 + \frac{\lambda_2}{2}\left(\frac{\partial Q_{ij3}}{\partial z}\right)^2 \right]. \tag{14}$$

This free-energy density is minimal for a uniformly absent threefold ordering ($Q_{ijk} = \partial Q_{ijk}/\partial z = 0$).

We introduce the decay lengths of this ordering: $\xi_4 = \sqrt{\lambda_1/A_1}$ and $\xi_5 = \sqrt{(5\lambda_1 + 3\lambda_2)/5A_1}$. Because the evolution of this type of ordering has not been studied before, we have no guessed values for these characteristic lengths. These lengths, however, are expected to be much shorter than the decay lengths of the nematic order since this surface-induced ordering does not normally occur in nematic liquid crystals.

Using Eqs. (12) and (13) and the decay lengths ξ_4 and ξ_5, we can write the free energy as

$$\frac{F_3(z)}{A_1} = 2[h(z)^2 + \xi_4^2 h'(z)^2] + 5[Q_{223}(z)^2 + \xi_5^2 Q'_{223}(z)^2]. \tag{15}$$

Minimizing this free energy and imposing the boundary conditions on Q_{ijk} at the substrate surface gives the solutions

$$h(z) = Q_A^{(3)} \exp[z/\xi_4], \tag{16}$$

$$Q_{223}(z) = -\frac{Q_{333}|_{z=0}}{2} \exp[z/\xi_5], \tag{17}$$

where we define $Q_A^{(3)} = \sqrt{Q_{122}|_{z=0}^2 + Q_{222}|_{z=0}^2}$.

D. Coupling between threefold and nematic order

So far, we have considered the threefold and nematic orderings to evolve independently from each other. In this section we add an interaction of the nematic ordering with the threefold ordering, by introducing a coupling term in the free energy. Such a coupling term is a rotational invariant contraction of the order-parameter tensors associated with different types of ordering. One can construct many coupling terms with tensors of second and third rank. The question arises which term gives a Ψ dependence of the free-energy expansion.

The lowest-order terms not involving any gradients and showing a Ψ dependence are

$$\sum_{i,j,k,l,m,n=1}^{3} Q_{ijk}Q_{lmn}Q_{ij}Q_{kl}Q_{mn}, \tag{18a}$$

$$\sum_{i,j,k,l,m,n=1}^{3} Q_{ijk}Q_{lmn}Q_{il}Q_{jm}Q_{kn}. \tag{18b}$$

Both terms have, apart from a constant term, a Ψ dependence of the interfacial energy of the form

$$\int_{-\infty}^{0} -\tfrac{1}{2}h(z)^2 g(z)^3 dz \cos 6\Psi = C_1 \cos 6\Psi. \tag{19}$$

$g(z)$ and $h(z)$ have been defined in Eqs. (9c) and (16), respectively. The extrema of this Ψ-dependent term lie at $\Psi = 0$ and $\pi/6$, with a period of $\pi/3$. Whether one of the extrema is a minimum (corresponding to an anchoring direction) or a maximum is determined by the sign of the coefficient C_1. For a negative (positive) C_1 this coupling term leads to anchoring directions parallel (perpendicular) to the mirror planes of the substrate.

The experimentally observed anchoring transitions correspond to a change of the location of the minima of the coupling term with the orientational order in the surface layer. With the present term, this can only be obtained if the coefficient C_1 changes sign as a function of the surface order. This coefficient C_1, however, is quadratic in $h(z)$ and cubic $g(z)$. Since the latter is independent of the surface order, this coupling term cannot give rise to any anchoring transition and C_1 cannot change sign as a function of the surface order. The terms given by Eq. (18) are obviously not relevant for the anchoring behavior we observe and can thus be neglected.

We consider therefore higher-order coupling terms

$$\sum_{i,j,k,l,m,n,p=1}^{3} Q_{ijk}Q_{lmn}Q_{ij}Q_{kl}Q_{mp}Q_{np}, \tag{20a}$$

$$\sum_{i,j,k,l,m,n,p=1}^{3} Q_{ijk}Q_{lmn}Q_{il}Q_{jm}Q_{kp}Q_{np}. \tag{20b}$$

Performing the summations (20) and not considering the Ψ-dependent terms yields, for both expressions,

$$\int_{-\infty}^{0} \tfrac{1}{2}Q_{33}(z)h(z)^2 g(z)^3 dz \cos 6\Psi = C_2 \cos 6\Psi. \tag{21}$$

The amplitude of $\cos 6\Psi$ in Eq. (21) is determined, apart from the factor $h(z)^2 g(z)^3$, by the component $Q_{33}(z)$ of the nematic order-parameter tensor. This factor $Q_{33}(z)$ can change the sign of C_2 if $Q_{33}|_{z=0}$ varies and therefore give rise to the anchoring transitions observed experimentally.

Performing the integration in Eq. (21) yields

$$\begin{aligned} C_2 = \frac{27}{16} Q_b^3 (Q_A^{(3)})^2 \Bigg\{ & \frac{Q_b \xi_4}{4} + \frac{3Q_b \xi_1 \xi_4}{4(\xi_1 \xi_4)} - \frac{3Q_b \xi_1 \xi_4}{2(\xi_1 \xi_4)} \\ & - \frac{(Q_b + 2Q_{33}|_{z=0})\xi_2 \xi_4}{2(2\xi_2 + \xi_4)} - \frac{3(Q_b + 2Q_{33}|_{z=0})\xi_1 \xi_2 \xi_4}{2(2\xi_1 \xi_2 + \xi_1 \xi_4 + \xi_2 \xi_4)} \\ & - \frac{3(Q_b + 2Q_{33}|_{z=0})\xi_1 \xi_2 \xi_4}{2(2\xi_1 \xi_2 + \xi_1 \xi_4 + \xi_2 \xi_4)} \\ & + \frac{(Q_b + 2Q_{33}|_{z=0})\xi_1 \xi_2 \xi_4}{2(2\xi_1 \xi_2 + \xi_1 \xi_4 + \xi_2 \xi_4)} \Bigg\}. \end{aligned} \tag{22}$$

Since ξ_4 is expected to be much smaller than ξ_1 and ξ_2, we perform a Taylor expansion of Eq. (22) in ξ_4/ξ_i ($i = 1,2$). After factorization, one gets

$$C_2=\frac{27}{16}\,Q_b^3(Q_A^{(3)})^2\,\frac{3\xi_4^4}{8\xi_1^3}\Bigg[Q_b\,\frac{\xi_4}{\xi_2}+Q_{33}|_{z=0}\Bigg(-1+3\,\frac{\xi_4}{\xi_1}+2\,\frac{\xi_4}{\xi_2}\Bigg)+O(\xi_4^2)\Bigg]. \tag{23}$$

The first factor in Eq. (23) cannot change the sign of C_2; however, the second factor does change sign for a certain value Q_{33}^c of $Q_{33}|_{z=0}$ with

$$Q_{33}^c=Q_b\xi_1\xi_4/(\xi_1\xi_2-3\xi_2\xi_4-2\xi_1\xi_4)\approx Q_b\xi_4/\xi_2. \tag{24}$$

The above coupling term thus gives rise to a reorientation of the bulk director driven by an evolution of the nematic order parameter $Q_{33}|_{z=0}$ around Q_{33}^c. Values of $Q_{33}|_{z=0}$ below Q_{33}^c result in a director parallel to the surface mirror planes. Above this critical value Q_{33}^c the director orients perpendicular to the mirror planes.

Using our experimental results, we an now estimate the range of ξ_4. Since we find experimentally that $Q_{33}|_{z=0}$ is always smaller than 0.02 (Fig. 8), Q_{33}^c must also be smaller than this limit, which means $0\leqslant\xi_4\leqslant Q_{33}^c\xi_2/Q_b\approx 0.4$ nm (taking $\xi_2\approx 10$ nm and $Q_b=0.6$). ξ_4 is indeed much smaller than ξ_2; it corresponds to one layer of molecules oriented parallel to the surface. As was anticipated, the surface-induced threefold order decays over a much smaller length scale than the nematic ordering.

E. Evolution of the orientational distribution in the interfacial region

In the previous sections we have determined the evolution of the order parameters of the nematic and threefold ordering in the interfacial region. The components of these order parameters are simply related to the coefficients of the expansion of the orientational distribution into spherical harmonics:

$$f(\theta,\phi,z)=\sum_{l=0}^{\infty}\sum_{m=-l}^{l}\langle Y_l^m(z)\rangle Y_l^m(\theta,\phi). \tag{25}$$

From our calculations, we know the spatial evolution of the coefficients correspnoding to $l=2,3$ [the other coefficients $\langle Y_l^m(z)\rangle|_{l=2,3}$are zero],

$$\langle Y_2^0(z)\rangle=\sqrt{\frac{5}{4\pi}}\,Q_{33}(z), \tag{26a}$$

$$\langle Y_2^{-1}(z)\rangle=-\langle Y_2^1(z)\rangle=\frac{1}{6}\sqrt{\frac{30}{\pi}}\,Q_{13}(z), \tag{26b}$$

$$\langle Y_2^{-2}(z)\rangle=\langle Y_2^2(z)\rangle=-\frac{1}{6}\sqrt{\frac{30}{\pi}}\Bigg(Q_{22}(z)+\frac{Q_{33}(z)}{2}\Bigg), \tag{26c}$$

$$\langle Y_3^0(z)\rangle=\frac{35}{4\sqrt{7\pi}}\,Q_{333}(z), \tag{26d}$$

$$\langle Y_3^{-3}(z)\rangle=-\frac{1}{2}\sqrt{\frac{35}{\pi}}[Q_{122}(z)+iQ_{222}(z)], \tag{26e}$$

$$\langle Y_3^3(z)\rangle=\frac{1}{2}\sqrt{\frac{35}{\pi}}[Q_{122}(z)-iQ_{222}(z)]. \tag{26f}$$

Since we do not know the other coefficients $\langle Y_l^m(z)\rangle$, we can only calculate that part of the expansion of $f(\theta,\phi,z)$ corresponding to $l=2,3$, which we will denote $\tilde{f}$. $\tilde{f}$ contains, however, the two most important components of the ordering for the anchoring behavior we want to describe. Since $\tilde{f}$ is not the complete distribution function, it can take negative values. To facilitate a spherical representation of $\tilde{f}$, we add for every z a positive constant to $\tilde{f}(\theta,\phi,z)$in such a way that the minimum of $\tilde{f}(\theta,\phi,z)$is zero.

As an example of how $\tilde{f}$ evolves with z in the case of bulk anchoring directions parallel and perpendicular to the preferred orientations of the surface molecules, Fig. 10 shows the evolution of $\tilde{f}$ in 7CB for partial vapor pressures of $\tilde{p}=0.2$ and 0.75. For $z=0$ Fig. 10 shows a distribution that resembles the distribution $f(\theta,\phi)$ determined with the maximum-entropy method from the second-harmonic generation measurements (Fig. 7) with the difference that the present plot shows only the part of the distribution corresponding to $\langle Y_l^m(z)\rangle$ components with $l=2,3$.

F. Summary of theoretical results

Our theoretical description of the behavior of nematic liquid crystals on a surface with a threefold symmetry leads to the following predictions. The conventional Landau–de Gennes model of the nematic order predicts that planar anchoring of the bulk nematic phase occurs if the scalar nematic order parameter $Q_{33}|_{z=0}$ at the surface is smaller than 0.07. For values of $Q_{33}|_{z=0}$ larger than this limit, homeotropic anchoring of the bulk phase is predicted. This is in agreement with our experimental observations as the experimentally measured surface order parameter $Q_{33}|_{z=0}$ did not exceed this value of 0.07 and only planar anchorings were observed. However, this model does not predict any preferred in-plane orientation for the bulk nematic liquid crystal. When the surface-induced threefold ordering is taken into account and coupled to the nematic ordering, our calculations show that the bulk director has the choice between three energetically equivalent in-plane orientations: The anchoring is tristable, as observed experimentally.

The bulk orientation can be either parallel or perpendicular to the surface mirror planes. Which case occurs is determined by the value of $Q_{33}|_{z=0}$. If $Q_{33}|_{z=0}$ decreases from a value larger than a certain threshold Q_{33}^c to a value smaller than Q_{33}^c, a first-order anchoring transition is induced at which the bulk director changes from an orientation perpen-

dicular to an orientation parallel to the mirror planes of the mica surface: This is what we have observed experimentally in 5OCB. In the case $Q_{33}|_{z=0}$ increases from below Q_{33}^c to above Q_{33}^c, the reverse anchoring transition is induced, which is what we have observed in 7CB.

The value $Q_{33}|_{z=0,c}$ is related to the decay length ξ_4 of the threefold ordering. From the experimentally determined ($Q_{33}|_{z=0,c} \leqslant 0.02$) we can estimate an upper limit for this decay length: $0 \leqslant \xi_4 \leqslant 0.4$ nm.

V. CONCLUSION

From the present study we can draw several conclusions concerning the anchoring behavior of 5OCB and 7CB on phlogopite mica, and, more generally, the anchoring mechanisms leading to multistable anchoring. Concerning the bulk anchoring directions, we have observed that 5OCB and 7CB orient differently on phlogopite mica. In a dry atmosphere, 5OCB orients perpendicular to the mirror planes of the mica surface, whereas 7CB orients parallel to these planes. If water vapor is added in the atmosphere surrounding the liquid crystal, both liquid crystals exhibit an anchoring transition where the bulk reorients in the plane parallel to the substrate. After this transition, 5OCB orients parallel to the surface mirrror planes, while 7CB orients perpendicular to these planes.

In contrast, the preferred alignment of the molecules in the surface layer in direct contact with the substrate is essentially independent of the liquid crystal and the presence of water vapor. The orientational distribution in the surface layer always exhibits four peaks. One peak is oriented perpendicular to the substrate, the other three peaks are oriented in the surface mirror planes on a cone of opening approximately 58° with respect to the surface normal.

The distribution of molecular orientations around these preferred directions shows, however, some evolution when the partial pressure of water in the atmosphere increases. In both 5OCB and 7CB, the in-plane anisotropy decreases. In contrast, the tilt distribution varies in opposite ways in the two compounds: The two order parameters $Q_{333}=\langle 3\cos\theta + 5\cos 3\theta\rangle/20$ and $Q_{33}=\langle(3\cos^2\theta-1)/2\rangle$ characterizing this tilt distribution decrease in 5OCB and increase in 7CB. This opposite variation of Q_{333} and Q_{33} in these two compounds can be put in parallel with the opposite variation of their bulk anchoring transition induced by adding water vapor. This strongly suggests that the in-plane reorientations of the bulk liquid crystal at the anchoring transitions are due to changes in the titlt distribution of the surface molecules instead of changes in their in-plane distribution.

These observations allow us to deduce an anchoring mechanism by which a substrate with a threefold symmetry or higher can induce several definite in-plane anchoring directions on a bulk liquid crystal. This mechanism involves two components of the orietational order: the uniaxial nematic order existing in the bulk of the liquid crystal and the surface-induced order with the symmetry of the substrate surface found in the surface layer of the liquid-crystal molecules. This surface-induced order extends over a certain distance from the surface that is significantly shorter than the coherence length of the nematic ordering. Because of the surface symmetry, the boundary conditions on the nematic order at the surface are isotropic in the plane. The nematic order gets oriented in the surface plane by a coupling to the surface-induced order that exists over the narrow interfacial region where both the nematic and surface-induced orders are present.

We have formalized this anchoring mechanism for the case of the phlogopite mica surface by extending the

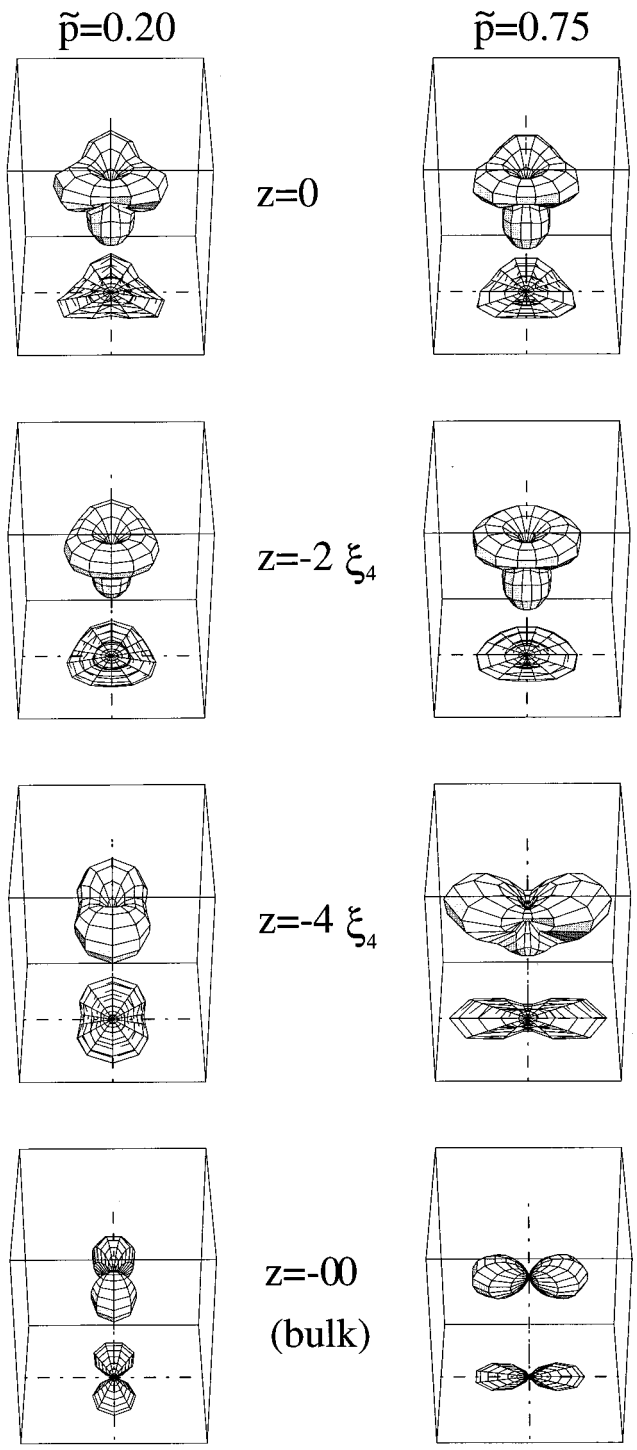

FIG. 10. Evolution of the function $\tilde{f}$ versus the distance z with respect of the surface ($z=0,-2\xi_4,-4\xi_4,-\infty$) for a bulk anchoring direction (a) parallel and (b) perpendicular to a mirror plane σ. ξ_4 has been set equal to $0.016\xi_2$.

Landau–de Gennes theory to take into account the surface-induced threefold component of the orientational order. By introducing a term coupling the nematic order to the surface-induced order in the free energy, we can account for all the bulk anchoring directions we have observed in 5OCB and 7CB using as the boundary conditions the experimentally measured orientational distributions in the surface layer. In particular, the observed variation of Q_{33} at the surface induces opposite anchoring transitions in 5OCB and 7CB between orientations perpendicular and parallel to the mirror planes of the mica surface.

ACKNOWLEDGMENTS

This work is part of the research program of the Stichting voor Fundamenteel Onderzoek der Materie, which is financially supported by the Nederlandse Organisatie voor Wetenschappelijk Onderzoek. We thank J. Chakrabarti, B. Mulder, and W. H. de Jeu for fruitful discussions.

[1] W. Gibbons, P. Shanon, S. T. Sun, and B. Svetlin, Nature (London) **351**, 49 (1991).
[2] M. Schadt, H. Seiberle, and A. Schuster, Nature (London) **381**, 212 (1996).
[3] V. Gupta and N. Abbott, Phys. Rev. E **54**, R4540 (1996).
[4] V. Gupta and N. Abbott, Science **276**, 1533 (1997).
[5] B. Jérôme, Rep. Prog. Phys. **54**, 391 (1991).
[6] W. Chen, M. Feller, and Y. Shen, Phys. Rev. Lett. **63**, 2665 (1989).
[7] M. Barmentlo, R. J. Hollering, and N. A. J. M. van Aerle, Phys. Rev. A **46**, R4490 (1992).
[8] D. Johannsmann *et al.*, Phys. Rev. E **48**, 1889 (1993).
[9] X. Zhuang, L. Marrucci, and Y. R. Shen, Phys. Rev. Lett. **73**, 1513 (1994).
[10] B. Jérôme, J. Phys.: Condens. Matter **6**, A269 (1994).
[11] B. Jérôme *et al.*, Phys. Rev. Lett. **71**, 758 (1993).
[12] B. Jérôme and Y. R. Shen, Phys. Rev. E **48**, 4556 (1993).
[13] The case of a twofold symmetry is intermediate and can be classified as low or high symmetry depending on the orientation of the surface director. If the surface director is parallel to the surface (which is allowed by symmetry), the situation is similar to that of the surfaces with a mirror symmetry and the induced anchoring is monostable. If the surface director is perpendicular to the surface, the situation is similar to that of surfaces with a threefold symmetry or higher and multistability may be induced.
[14] F. Grandjean, Bull. Soc. Fr. Mineral. Cristallogr. **39**, 164 (1916).
[15] N. Tikhomirova and A. Guinsberg, in *Advances in Liquid Research and Applications*, edited by L. Bata (Pergamon, Oxford, 1980), p. 651.
[16] E. Frolova, O. Sarbey, and A. Sybashvily, Mol. Cryst. Liq. Cryst. **104**, 111 (1984).
[17] T. Korkishko *et al.*, Sov. Phys. Crystallogr. **32**, 263 (1987).
[18] B. Jérôme, A. Bosseboeuf, and P. Pieranski, Phys. Rev. A **42**, 6032 (1990).
[19] P. Pieranski, B. Jérôme, and M. Gabay, Mol. Cryst. Liq. Cryst. **179**, 285 (1990).
[20] P. Pieranski, Liq. Cryst. **5**, 683 (1989).
[21] Y. R. Shen, Nature (London) **337**, 519 (1989).
[22] K. B. Eisenthal, Annu. Rev. Phys. Chem. **43**, 627 (1992).
[23] T. F. Heinz, in *Nonlinear Surface Electromagnetic Phenomena*, edited by H. E. Ponath and G. Stegeman (Elsevier Science, Amsterdam, 1991), Chap. 5, pp. 353–416.
[24] M. B. Feller, W. Chen, and Y. R. Shen, Phys. Rev. A **43**, 6778 (1991).
[25] E. T. Jayne, Phys. Rev. **106**, 620 (1957).
[26] *Micas*, Vol. 13 of *Reviews in Mineralogy*, edited by S. W. Bailey (Bookcrafters, Chelsea, 1987).
[27] G. Friedel, *Leçons de Cristallographie* (Librarie Scientifique Albert Blanchard, Paris, 1964), p. 420.
[28] Merck, datasheets supplied with liquid crystals 5OCB and 7CB.
[29] P. Pieranski and B. Jérôme, Phys. Rev. A **40**, 317 (1989).
[30] P. de Gennes, Mol. Cryst. Liq. Cryst. **12**, 193 (1971).
[31] We have also calculated the evolution of the tensor Q_{ijk} in the general case wihtout imposing *a priori* a threefold symmetry at any z. As expected, if we impose on this general solution the boundary conditions at $z=0$ with the threefold of the surface layer, the tensor Q_{ijk} conserves this threefold symmetry for any z.
[32] In principle, other gradient terms should be added to our expression of F_3. However, each of these terms is associated with an unknown coefficient. Since we focus on the effect of the coupling between nematic and threefold order, we keep the number of gradient terms (and therefore unknown parameters) limited.